

Published in final edited form as:

J Comp Neurol. 2010 August 15; 518(16): 3272–3289. doi:10.1002/cne.22399.

Molecular analysis of neocortical layer structure in the ferret

Joanna J. Rowell, Atul K. Mallik, Jennifer Dugas-Ford, and Clifton W. Ragsdale

Department of Neurobiology, The University of Chicago, 947 East 58th Street Chicago, IL 60637, USA

Abstract

Molecular markers that distinguish specific layers of rodent neocortex are increasingly employed to study cortical development and the physiology of cortical circuits. The extent to which these markers represent general features of neocortical cell type identity across mammals is, however, unknown. To assess the conservation of layer markers more broadly, we isolated orthologs for fifteen layer-enriched genes in the ferret, a carnivore with a large, gyrencephalic brain, and analyzed their patterns of neocortical gene expression. Our major findings are: (1) Many but not all layer markers tested show similar patterns of layer-specific gene expression between mouse and ferret cortex, supporting the view that layer-specific cell type identity is conserved at a molecular level across mammalian superorders; (2) Our panel of deep layer markers (*ER81/ETV1*, *SULF2*, *PCP4*, *FEZF2/ZNF312*, *CACNA1H*, *KCNN2/SK2*, *SYT6*, *FOXP2*, *CTGF*) provides molecular evidence that the specific stratifications of layer 5 and 6 into 5a, 5b, 6a and 6b are also conserved between rodents and carnivores. (3) Variations in layer-specific gene expression are more pronounced across areas of ferret cortex than between homologous areas of mouse and ferret cortex; (4) This variation of area gene expression was clearest with the superficial layer markers studied (*SERPINE2*, *MDGA1*, *CUX1*, *UNC5D*, *RORB/NR1F2*, *EAG2/KCNH5*). Most dramatically, the layer 4 markers *RORB* and *EAG2* disclosed a molecular sublamination to ferret visual cortex and demonstrated a molecular dissociation among the so-called agranular areas of the neocortex. Our findings establish molecular markers as a powerful complement to cytoarchitecture for neocortical layer and cell-type comparisons across mammals.

Keywords

Mouse; visual cortex; motor cortex; cingulate cortex; cytoarchitecture; corticospinal motor neuron; *SERPINE2*; *MDGA1*; *UNC5D*; *CUX1*; *EAG2*; *RORB*; *ER81*; *PCP4*; *SULF2*; *FEZF2*; *CACNA1H*; *KCNN2*; *FOXP2*; *SYT6*; *CTGF*

INTRODUCTION

The six-layered cerebral cortex, or neocortex, is a conserved feature of the dorsal telencephalon of all mammals, including the marsupials and monotremes (Northcutt and Kaas, 1995). That the neocortex is stratified is clear from almost any histological preparation, but the specific identification of six neocortical layers is a historical consensus. The Viennese anatomist Meynert (1872) was the first to describe cell-rich neocortical layers, and he recognized five layers in the human brain. Subsequently, the English neurologist Lewis (1880; 1882; 1878) suggested a division of the cortex into six layers based on the cytoarchitecture of pig, sheep, rat, rabbit and cat brains, and Ramon y Cajal (1899–1904) described between 7 – 9 layers in the human cortex, the number depending on the cortical

area studied. In 1903 Brodmann adopted and popularized Lewis' diagram and, through his advocacy, the concept of 'six layers' swept the field (Lorente de No, 1943).

The historical disagreement over the number of cortical layers highlights the challenges of using cytoarchitecture to identify neocortical layers and cell types. Lorente de No (1943) was particularly critical of cytoarchitectonics even for layer identification because of the publication of "most inconsistent descriptions" of cortical layers. "(T)he boundaries between layers, with the exception of the boundary between IVb and V, are never sharp, and ... if they are ascertained with the help of only the architectonic picture are entirely hypothetical" (Lorente de No, 1943, pp 278–279). Cytoarchitecture is also problematic for cortical cell type identification. Cortical cytoarchitectonics is based on quantitative differences between populations of neurons, such as their packing densities and the relative local percentages of pyramidal neurons. It is not a method that studies specific properties of individual cells. Indeed, it is the population-based analysis of cytoarchitecture that made this method so adaptable to layer comparisons across cortical areas and species.

Cortical layering can be demonstrated with other methods, including single cell tract-tracing anatomy and single unit electrophysiology (Gilbert, 1977; Gilbert and Kelly, 1975; Gilbert and Wiesel, 1985; Jones and Wise, 1977; Lund et al., 1975; Symonds and Rosenquist, 1984). These studies have shown that layers serve to organize neocortical afferent connections, local circuitry, and output projections. One advantage of these studies is that they identify specific cell types at specific locations. Unlike cytoarchitectonics, however, experimental tract-tracing and electrophysiology do not allow study of layering patterns across the whole of the neocortex.

A critical recent advance in the study of cortical layering is the discovery in the rodent of molecular markers with apparent layer-specific expression patterns (Hevner et al., 2003; Leone et al., 2008; Molyneaux et al., 2007). These layer markers represent a wide variety of protein products, and have been gradually identified over the past decade from the work of a number of groups (Table 1). For example, interest in neocortical neuron development led to the characterization of the zinc finger transcription factor *Fezf2* as a layer 5 marker (Arlotta et al., 2004; Chen et al., 2005; Inoue et al., 2004; Molyneaux et al., 2005). Interest in physiological properties of the neocortical neurons led to the discovery that the potassium channel *Eag2/Kcnh5* is enriched in layer 4 neurons (Ludwig et al., 2000; Saganich et al., 1999). A paramount but largely unexplored consequence of molecular markers for layer-enriched cell types is that it allows for study of populations of defined cortical cell types, which can address long-standing questions involving neocortical structure. These questions include whether excitatory neuronal subtypes are organized into layers divided by sharp boundaries (Lorente de No, 1943), what the full extent of cell type heterogeneity is within the neocortex (Bannister, 2005; Hevner et al., 2003; Masland, 2004; Nelson et al., 2006), and how variable the organization of neocortical layers is across cortical areas and mammalian species. A widely accepted but also deeply controversial hypothesis is that the neocortex is a relatively uniform tissue (Herculano-Houzel et al., 2008; Hutsler et al., 2005; Rakic, 2008; Rockel et al., 1980; Rockland and Ichinohe, 2004; Skoglund et al., 1996). Gene expression studies of layer markers allow a new approach to testing the hypothesis of neocortical uniformity across mammals.

To date, layer markers have been characterized in rodent brains and, to a lesser extent, in primate brains including the macaque and human (Hevner, 2007; Watakabe et al., 2007). We chose the ferret brain for comparative analysis for several reasons. First, unlike the mouse or rat, the ferret has a large, gyrencephalic brain (Smart and McSherry, 1986). Second, ferrets have been widely employed to study the development and the functional organization of neocortical sensory areas, particularly visual cortex (Bizley et al., 2005; Callaway and

Lieber, 1996; Crowley and Katz, 2000; Frantz and McConnell, 1996; Law et al., 1988; Manger et al., 2002; Pallas et al., 1990; Ware et al., 1999). Third, according to recent genomic and fossil data, primates and rodents are found in the same mammalian superorder (Euarchontoglires) with carnivores placed in a separate superorder (Laurasiatheria) (Fig. 1) (Goloboff et al., 2009; Lindblad-Toh, 2004; Lunter, 2007; Madsen et al., 2001; Murphy et al., 2001). As the ferret is more distantly related to rodents than to primates, the ferret is an excellent outgroup to test conservation of gene expression patterns across a wide subset of mammals. In particular, similarities between ferret and rodent will likely hold for humans as well.

Our results demonstrate both broad uniformity and substantial variation to the molecular cell type composition of the cortical layers across mammalian species and cortical areas. Primary sensory areas showed strikingly similar layer marker expression patterns between ferret and mouse. By contrast, across ferret cortical areas, we observed substantial variability in upper layer marker gene expression. These results indicate that the structure of the neocortical layers is more variable across cortical areas in the ferret than between homologous areas of ferret and mouse brain. We also provide evidence for molecular sublamination to ferret layers 2/3, 5 and 6, and for layer 4 in ferret visual cortex. This study demonstrates the utility of molecular markers for neocortical layer and cell type characterization, and endorses molecular architectonics as a powerful addition to conventional cytoarchitectonics for neocortex research.

MATERIALS AND METHODS

Animals and Tissue

Adult male and female ferrets (*Mustela putorius furo*) were obtained from Marshall Farms (North Rose, NY). Ferrets were deeply anesthetized with sodium pentobarbital and perfused through the heart with 200 ml 0.1M phosphate-buffered saline (PBS, pH = 7.4) followed by 500 ml 4% paraformaldehyde in PBS (PFA). Adult female CD-1 mice were deeply anesthetized and perfused through the heart with 40 ml PFA. With both mice and ferrets, dissected brains were immersed in PFA overnight, and fixed tissue was cryogenically protected by equilibration in 30% sucrose/PFA for 48hrs. Coronal sections were cut at 32 μ m on a sledge microtome. Sections were mounted on Superfrost Plus slides (Fisherbrand). Tissue was allowed to dry before processing for in situ hybridization. All animal procedures were reviewed and approved by the IACUC of the University of Chicago.

In situ hybridization (ISH)

PCR primers targeting ferret genes were designed with MacVector software based on dog genome sequence (Supplemental Table 1). Mouse cDNAs were published reagents obtained from colleagues, or were isolated by PCR based on deposited sequence (Supplemental Table 2). PCR fragments ranging in size from 350 – 1200 bp were subcloned in pCRII-TOPO vector (Invitrogen). Digoxigenin(DIG)-labeled riboprobes were synthesized from cDNA plasmids by in vitro transcription. Single-color ISH was carried out as previously described (Grove et al., 1998). Slides were incubated for 15 minutes in PFA, washed three times in PBS for 5 minutes, and incubated in proteinase K solution (1 μ g/ml of proteinase K in 100mM Tris-HCl, pH = 8.0; 50mM EDTA, pH = 8.0) for 1 hour (ferret tissue) or for 30 minutes (mouse tissue) at 37°C. Sections were post-fixed for 15 minutes in PFA, washed three times in PBS for 5 minutes, and prehybridized for 1 hour at 72°C in hybridization solution (200 μ g/ml heparin; 12.5mg/ml yeast RNA; 5 \times SSC; 1% SDS; 50% formamide). Following prehybridization, 0.5 – 2 μ g of RNA probe was added to the hybridization solution and incubated overnight at 72°C. After hybridization, slides were washed three times in Solution \times (2 \times SSC; 1% SDS; 50% formamide) for 45 minutes at 72°C, rinsed

three times in TBST (250mM Tris HCl, pH = 7.5; 1.36M NaCl; 26.8 mM KCl; 1% Tween 20) for 15 minutes at room temperature, and blocked in 10% lamb serum in TBST for one hour at 4°C. Riboprobe-mRNA duplexes were detected with Fab fragments coupled to alkaline phosphatase (Roche). The antibody was preabsorbed with chick embryo power/1% lamb serum and added to tissue at a 1:5000 dilution in TBST/1% lamb serum. The antibody reaction proceeded overnight at 4°C. The tissue was washed in TBST and then in NTMT (100mM Tris HCl, pH = 9.5; 100mM NaCl; 50mM MgCl₂; 1% Tween 20). The riboprobe-mRNA duplexes were detected by phosphatase histochemistry employing BCIP and nitro blue tetrazolium (NBT). After 1 – 5 days incubation, slides were rinsed, postfixed and coverslipped with Eukitt mounting medium.

Two-color fluorescence ISH

Two-color fluorescence ISH (FISH) was carried with DIG-, fluorescein (FL)-, or 2,4-dinitrophenol (DNP)- labeled riboprobes. In all cases, probes were hybridized in a single reaction, but were detected sequentially. After high-stringency washes the tissue was blocked in TBST/B (20% DIG Blocking solution from Roche in TBST). Riboprobe-mRNA duplexes were incubated for 2 hours at room temperature with anti-DIG, anti-DNP or anti-FL horseradish peroxidase antibodies at a final concentration of 1:200 in TBST/B. These antibodies were not preabsorbed. After antibody reaction, slides were washed three times in TBST for 15 minutes, and then washed twice in TNT (0.1M Tris HCl, pH = 7.5; 0.15M NaCl; 0.05% Tween 20) for five minutes. Signal was demonstrated by incubation with FITC, Cy3 or Cy5 tyramide dyes (1:50 in 1× Plus Amplification Diluent, Perkin-Elmer) for one hour at room temperature. Slides were washed three times in TNT for 15 minutes at room temperature, washed two times in detergent mix (1% Nonidet P-40; 1% SDS; 0.5% Deoxycholate; 50mM Tris-HCl, pH = 7.5; 1mM EDTA, pH = 8.0; 150 mM NaCl) for 15 minutes at 72°C, washed for 30 minutes in Solution × at 72°C, and washed three times in TBST for 15 minutes at room temperature. The slides were blocked again in TBST/B before antibody application in the second color. After fluorescence processing, the slides were rinsed in PBS and coverslipped in ProLong Gold Antifade Reagent (Invitrogen).

Antibody Characterization

Please see Supplemental Table 3 for a list of the four commercial antibodies employed in this study. The antibodies bind digoxigenin, 2,4-dinitrophenyl and fluorescein, which are not endogenous to vertebrate tissue. To test for nonspecific binding of the antibodies to ferret and mouse brain sections, we performed control experiments in which the labeled RNA was omitted from the hybridization mix (Supplemental Figure 1). No signal was detected in the absence of the hapten-labeled riboprobe, demonstrating that the antibodies react specifically with the synthetic RNA.

Microscopy

Single color tetrazolium sections were studied on an Axioskop 40 Microscope (Zeiss). Fluorescent signals were imaged on a TIRF Live Cell Microscope (Olympus), a DSU Fixed Sample Spinning Disk Confocal Microscope (Olympus) or a SP5 2-Photon Confocal Microscope (Leica). Images were processed with Photoshop CS3 and ImageJ, where the hue, saturation, brightness, and contrast were altered as necessary. For documentation where the image did not fall within the field of view of the microscope, two images were captured and stitched together using Photoshop CS3 (see Figure Legends).

Technical considerations

Direct comparisons of NBT and fluorescence ISH results established that the NBT technique was uniformly more sensitive than the fluorescent techniques. For example, single color

NBT data indicated that ferret *PCP4* was expressed throughout layer 5, but *PCP4* fluorescence signal could only be detected in the lower part of layer 5, where the *PCP4* message was stronger (compare Fig. 5B to 6A'). We concluded that the FISH technique failed to detect sites of low expression. Accordingly, we did not calculate coexpression percentages for FISH pairwise comparisons because these numbers would be fundamentally misleading. Positive FISH coexpression data are, however, reliable and are reported in the Results.

RESULTS

Molecular markers of neocortical layers in mouse

The goal of this study is a comprehensive comparison of layer marker gene expression patterns across mammalian species. To this end we identified a panel of candidate layer markers to study in ferret neocortex based on gene expression patterns reported in rodent brains (Table 1). In addition we isolated a subset of these markers in the mouse to allow for direct comparison of message distributions using identical in situ hybridization (ISH) protocols. Figure 2 depicts our results for mouse visual cortex. As expected from published reports, we found that *Cux1* and *Unc5d* were expressed in layers 2 – 4 (Fig. 2A,B), *Eag2* and *Rorb* showed enhanced expression in layer 4 (Fig. 2C,D), *Er81* message selectively labeled neurons in layer 5 (Fig. 2E), *Pcp4* ISH labeling was pronounced throughout layers 5 and 6 (Fig. 2F), *Fezf2* ISH showed heavy labeling in deep layer 5 and deep layer 6 (Fig. 2G), *Cacnalh* expression was concentrated in deep layer 5 (Fig. 2H), *Sulf2* message was enriched in layer 5 and deep layer 6 (Fig. 2I), *Foxp2* and *Syt6* expression was pronounced in layer 6 (Fig. 2J,K), and *Ctgf* selectively identified neurons in deep layer 6 (Fig. 2L). These results indicate that layer marker expression in mice is remarkably specific for, but seldom restricted to, individual cortical layers. For example, with our methods the layer 4 markers *Eag2* and *Rorb* identified many neurons in layer 5 (Fig. 2C,D), and the layer 6 marker *Foxp2* labeled cells throughout the cell-rich layers (Fig. 2J). The expression patterns reported here for mouse are similar to those of the Allen Mouse Brain Atlas, a gene expression database (www.brain-map.org; Lein et al., 2007; Ng et al., 2009; Ng et al., 2010). A detailed comparison of our findings with Allen Brain Atlas images can be found in Supplemental Table 4.

Molecular identification of neocortical layers in ferret

We isolated cDNAs for fifteen candidate layer markers in the ferret (Table 1). To identify cytoarchitectonic laminar patterns in ferret neocortex, we also isolated genes commonly employed as molecular markers for broad subsets of cortical neurons. This included *ELAVL3*, a pan-neuronal marker, *VGLUT1*, a marker of excitatory neurons, and *NEFM*, which is expressed strongly in medium to large neocortical pyramidal cells (see Table 1). We examined the expression patterns of these genes in sections of adult ferret tissue by single color ISH. We found that *ELAVL3*, *VGLUT1* and *NEFM* identified neocortical layers with varying degrees of clarity (Fig. 3A – C). *ELAVL3* expression (Fig. 3A) most closely resembled a Nissl stain, but proved less informative than *VGLUT1* and *NEFM* for layer identification. As illustrated in Figure 3 for ferret visual cortex, *VGLUT1* and *NEFM* ISH identified a layer 2/3 containing pyramidal cells which increased in size and packing density with cortex depth, a layer 4 marked by its dense packing of small non-pyramidal cells, a layer 5 consisting of the largest but least densely packed pyramidal cells, and a layer 6 that in comparison with layer 5 contained smaller and more densely packed cells (Fig. 3B,C). As expected, the *GAD65*-rich inhibitory neurons were scattered throughout the neocortical layers and white matter and showed little lamination (Fig. 3D, Feldblum et al., 1993; Gabbott and Somogyi, 1986). We conclude that among these four genes *NEFM* is the most

informative molecular marker for identifying ferret neocortical layers based on cytoarchitecture.

We employed two-color fluorescence in situ hybridization (FISH) in adult ferret tissue to determine whether candidate ferret layer marker genes are expressed in the predicted cytoarchitecturally defined layers. We found that the candidate ferret layer 4 marker *RORB* was expressed in the laminar territory identified as layer 4 by a marked reduction in *NEFM* expression (Fig. 3F). Similarly, candidate ferret layer 5 marker *ER81* and layer 6 marker *SYT6* were expressed in layers 5 and 6 of the ferret cortex as defined by *NEFM* cytoarchitecture (Fig. 3G,H). These data establish that ferret orthologs of key mouse layer marker genes are enriched in the corresponding layers of the ferret neocortex.

Layer 4 of ferret visual cortex is stratified

We isolated two candidate layer 4 markers, *RORB* and *EAG2*, and found both genes to be expressed in layer 4 of ferret neocortex across many regions of cortex (Fig. 4). These included primary motor cortex, an area that is classically described as agranular and where the identification of a layer 4 by cytoarchitecture is challenging (Fig. 4D–F). Throughout much of ferret neocortex, the expression of *RORB* and *EAG2* was dense in layer 4 but extended into layers 2/3 and 5 (Fig. 4A – F). Unexpectedly, we found *EAG2* expressed in upper layer 6 (Fig. 4C,D,F). The cat receives substantial dorsal thalamic input to layer 4 and upper layer 6 (Ferster and LeVay, 1978; LeVay and Gilbert, 1976), raising the possibility that in ferret *EAG2* identifies thalamorecipient cells more broadly.

Single-color ISH suggested that *EAG2* and *RORB* expression patterns were not coextensive in ferret primary visual cortex (Fig. 4B,C). *RORB*-rich neurons were more densely packed than *EAG2*-rich neurons, and *EAG2* expression was shifted superficially relative to *RORB* expression (Fig. 4B,C). We confirmed in two-color FISH experiments with *EAG2* and *RORB* that there is a layer 4 sublamination of ferret visual cortex with a *RORB*⁺/*EAG2*⁺ center, and a deep layer 4 that is *RORB*-rich and nearly free of *EAG2*-positive cells (Fig. 4G – G'', Supplemental Figure 2A – C). We found that the intensity of *EAG2* fluorescence peaks in upper layer 4, and gradually drops off in layer 2/3 above and in layer 4 below. By contrast, *RORB* fluorescence intensity in layer 4 increases with depth, peaks at the bottom of layer 4, but drops off rapidly beyond the layer 4 – 5 boundary (Supplemental Figure 2D). Thus, with our methods, *EAG2* and *RORB* mRNA appeared to be present in opposing gradients in layer 4 of ferret primary visual cortex.

In mouse visual cortex, no similar sublamination was evident (Fig. 4H – H'', Supplemental Figure 2M – P), suggesting that the layer 4 sublamination in visual cortex is a species-specific trait. Layer 4 sublamination was detected but was less pronounced in ferret primary somatosensory cortex (Supplemental Figure 2E – H), and was not seen in ferret motor cortex (Supplemental Figure 2I – L). These molecular findings raise the possibility that there may be a functional subdivision to layer 4 of ferret primary visual cortex.

'Layer 5' molecular markers are expressed in layers 5 and 6 of ferret cortex

Many layer 5 markers have been reported in the mouse. We isolated six of these layer 5 markers in the ferret: *ER81*, *PCP4*, *SULF2*, *FEZF2*, *CACNA1H* and *KCNN2*. Single color ISH demonstrated heterogeneous expression patterns of these markers in both layer 5 and layer 6 of ferret neocortex (Fig. 5). *ER81*, *PCP4*, and *SULF2* were expressed broadly within layer 5, and consistently identified a clear boundary between layers 4 and 5 (Fig. 5A – C). *ER81* was expressed throughout layers 5 and 6 (Fig. 3G, Fig. 5A), and *SULF2* and *PCP4* ISH labeled layer 5 and deep layer 6, with only weak expression in upper layer 6 (Fig. 5B, C).

In a variety of mammalian species layer 5 has been divided into two sublamina, 5a and 5b, based on cytoarchitectonics and connectivity (Lund et al., 1979; Lund et al., 1975). In ferret a similar cytoarchitectonic sublamination to layer 5 was evident, with deep layer 5 (5b) containing markedly larger pyramidal neurons than upper layer 5 (5a) (Fig. 3G, arrowhead). Layers 5a and 5b differed molecularly, with *FEZF2*, *CACNA1H* and *KCNN2* demonstrating strong expression in large pyramidal neurons in layer 5b (Fig. 5D – F). Expression of these genes was not restricted to layer 5b. *FEZF2* was also expressed weakly in layer 5a and upper layer 6 (Fig. 5D), *CACNA1H* message was demonstrated in upper layer 6 and layers 2/3 (Fig. 5E), and *KCNN2* ISH identified upper layer 6 (Fig. 5F). In mouse *FEZF2*, *CACNA1H*, and *KCNN2* were also expressed strongly in deep layer 5 (Figure 2G,H and Supplemental Figure 3), indicating a shared molecular sublamination to layer 5 between mouse and ferret.

Layer 5 sublamination studied in motor cortex

We explored the molecular architecture of layer 5 in motor cortex with two-color FISH. For these experiments *SULF2* gene expression proved to be particularly valuable because it identified all of layer 5 and, by its reduced expression in upper layer 6, it clearly demarcated the boundary between layers 5 and 6 (Fig. 5C, 6). We found *PCP4* and *SULF2* to be extensively coexpressed in layer 5b and deep layer 6 (Fig. 6A – A''). While *SULF2* expression levels were strong throughout layer 5, we found that *PCP4* expression in layer 5a was undetectable using the less sensitive FISH technique (Fig. 6A', A''), molecularly distinguishing a layer 5a and layer 5b. Two-color FISH with *ER81* and *SULF2* demonstrated that *ER81* is expressed weakly in layer 5a, but strongly labels large cells in deep layer 5 and upper layer 6 (Fig. 6B – B'').

We tested the extent of *FEZF2*, *CACNA1H*, and *KCNN2* mRNA coexpression in layer 5b of ferret motor cortex with two-color FISH. *FEZF2* and *CACNA1H* colocalized with *SULF2* in large, pyramidal-shaped neurons in layer 5b (Fig. 6C – C'', E – E''). Pairwise comparisons not involving *SULF2* directly demonstrated extensive coexpression of *FEZF2* and *CACNA1H* (Fig. 6D – D'') and of *CACNA1H* and *KCNN2* (Fig. 6F – F'') in layer 5b. This suggests that layer 5b features a neuronal subtype characterized by combined *FEZF2/CACNA1H/KCNN2* expression. Interestingly, *CACNA1H* and *KCNN2* were expressed in non-overlapping punctate patterns, suggesting that the mRNAs of these ion channel genes are localized to distinct subcellular compartments (Fig. 6F'').

Molecular identification of layers 6a and 6b

Two candidate layer 6 markers showed strong patterned expression in the adult ferret neocortex. Single color ISH demonstrated that *SYT6* was expressed in layer 6 and scattered layer 5 neurons throughout the cortex, including primary visual and motor areas (Fig. 7A,C). *FOXP2* expression in primary visual cortex was enriched in layer 6 with conspicuous expression throughout the cell-rich layers (Fig. 7B), whereas in motor cortex *FOXP2* was expressed more evenly with very little layer 6 selectivity (Fig. 7D). These results establish *SYT6* as a more specific layer 6 marker than *FOXP2* in ferret.

Two-color FISH experiments demonstrated a molecular sublamination to layer 6, with *EAG2* and *SYT6* mRNA expressed in layer 6a, and *SULF2* and *PCP4* message enriched in layer 6b (Fig. 7E – G''). This dissociation was not absolute, as we saw scattered *SYT6*+ neurons in layer 6b, and weakly expressing *SULF2*+ neurons in layer 6a (Fig. 7E – E''). Two-color FISH experiments demonstrated that *SYT6* and *EAG2* mRNA were broadly coexpressed within layer 6a (Fig. 7G – G''), and that *SULF2* and *PCP4* were broadly coexpressed within layer 6b (Fig. 6A – A'').

In the cat a laminar subdivision of layer 6 has been identified based on cell morphology (Peters and Yilmaz, 1993). We found that our molecular results correlate with a similar cytoarchitectonic sublamination in ferret, as *SYT6* and *EAG2*-rich neurons in layer 6a were often pyramidal in shape, while *SULF2*-rich neurons in layer 6b were typically fusiform in shape. We confirmed that the fusiform neurons were excitatory by demonstrating coexpression of *VGLUT1* with both *SULF2* and *PCP4* in layer 6b (Figure 7K–L").

There is a similar subdivision of layer 6 in the mouse neocortex, with the expression of *Syt6* in the pyramidal neurons of layer 6a and *Ctfg* and *Sulf2* in the fusiform neurons of layer 6b (Fig. I, K, L and Supplemental Figure 4), often called the subplate (Allendoerfer and Shatz, 1994). In ferret we found that *CTGF* was not expressed strongly or selectively in layer 6b, but was found in scattered cells throughout the neocortical layers with modest layer 6 selectivity (Supplemental Figure 5). In addition, *Eag2* was only weakly expressed in the upper part of layer 6 in the mouse neocortex (Supplemental Table 4), not strongly as in ferret. These results indicate that there is a conserved subdivision of layer 6 across ferret and mouse, with important differences in their molecular characteristics.

In ferret, *SYT6* was expressed densely in layer 6a, in scattered cells in layer 6b and in cells in the underlying white matter (Fig. 7H – J"). Very few VGLUT1+ neurons were detected in the white matter with the sensitive NBT ISH protocol (Supplemental Figure 6A), which suggested that the deep SYT6+ cells might be inhibitory neurons. To test this possibility directly we performed two color FISH for *SYT6* with *GAD65* (Fig. 7H – J") and *VGLUT1* (Supplemental Figure 6B – B"). In layer 6a, *SYT6*+ neurons expressed *VGLUT1* mRNA and not *GAD65* message (Fig. 7I – I" and Supplemental Figure 6B – B"). Deep white matter *SYT6*+ cells, by contrast, were *GAD65*-rich (Fig. 7J – J"). These results establish that cortical *SYT6*-rich neurons are a heterogeneous population, and include excitatory neurons within layer 6a and inhibitory neurons in the cortical white matter (Higo et al., 2007; Rockland, 1985).

Expression of superficial layer markers is particularly selective for layers 2/3 in sensory cortex

We isolated four genes that labeled neurons in layers 2/3 in ferret: *CUX1*, *UNC5D*, *SERPINE2*, and *MDGA1* (Fig. 8). We found that *UNC5D* and *CUX1* showed substantial variability in their expression patterns across ferret neocortical areas. In visual cortex, *CUX1* was expressed throughout layers 2 – 4 (Fig. 8E), and *UNC5D* expression was strongest in layer 2/3 (Fig. 8D). This selectivity for upper layer gene expression, also present in somatosensory cortex (Fig. 8I,J), was greatly reduced in ferret motor cortex (Fig. 8N,O) and in other, non-sensory cortical areas (Fig. 9D). These results establish that there is a concentration in ferret sensory areas of upper layer cells that strongly express *CUX1* and *UNC5D*.

We isolated *MDGA1* and *SERPINE2* cDNA fragments because these genes were reported in mouse to identify layer 4 (*Mdga1*) and layer 5 (*Serpine2*) of sensory cortex (Reinhard et al., 1994; Takeuchi et al., 2007). In ferret primary sensory areas, we found that *MDGA1* and *SERPINE2* showed enhanced expression in a band of cells just underneath the molecular layer (Fig. 8). We saw very few *MDGA1*+ neurons in layer 4 of ferret primary visual cortex (Fig. 8C) or somatosensory cortex (Fig. 8H), but we did observe low-level expression of *MDGA1* in layer 6 (Fig. 8C,H,M). *SERPINE2* was expressed in scattered cells throughout the neocortex, with only modest enrichment in layer 5 of somatomotor cortex (Fig. 8B,G,L). Thus, the most pronounced gene expression pattern for these markers in ferret neocortex was strong expression in upper layer 2/3, which potentially distinguishes a layer 2 from 3. This point deserves further investigation as additional layer 2/3 markers are identified (Molyneaux et al., 2009).

Expression patterns of upper layer markers in medial limbic neocortex

Carnivore neocortex has extensive non-sensory and motor districts that are well characterized by cytoarchitectonics and tract-tracing anatomy. We examined layer marker gene expression patterns in one such district, the medial limbic cortex. In the cat, this region is broadly subdivided into the anterior and posterior limbic areas (Brodmann, 1909; Krettek and Price, 1977; Rose and Woolsey, 1948). The anterior limbic area is agranular, whereas the posterior limbic area contains the granular posterior cingulate cortex, and the agranular and granular retrosplenial areas. We found that the expression patterns of three superficial layer markers, *EAG2*, *RORB*, and *CUX1*, readily distinguished these areas of medial limbic cortex.

In the agranular anterior limbic area, *EAG2* expression in layer 6 was maintained, but that in layer 4 was dramatically reduced (Fig. 9A,B). By contrast, layer 4 *RORB* expression was robust (Fig. 9C). These results indicate a layer 4 can be identified with the molecular marker *RORB* in anterior limbic cortex, but that the reduction of granularity here is accompanied a loss of layer 4 *EAG2* expression.

In the posterior limbic cortex, gene expression identified a clear boundary between the posterior cingulate and agranular retrosplenial areas. In layer 4 of the granular posterior cingulate area *EAG2* and *RORB* expression was strong. With the transition into the ventrally adjoining agranular retrosplenial area, *EAG2* expression in layer 4 split into two separate bands (Fig. 9G), *RORB* expression was dramatically reduced (Fig. H), and *CUX1* expression in superficial layers increased in density but decreased in thickness (Fig. 9I). Finally, in all medial limbic areas examined, including the anterior limbic cortex, deep layer marker expression patterns appeared unchanged in comparison to the patterns seen in sensory and motor areas (Fig. 9E,J).

DISCUSSION

Our results on the molecularly defined cell type composition of neocortical layers in the adult ferret and mouse visual cortex are summarized in Figure 10. As a general finding, gene expression patterns proved to be broadly conserved between rodents and carnivores, supporting evolutionary constancy in the cell type composition of the neocortical layers. In detailed examination, however, we identified substantial expression pattern variability across species and cortical areas. Across mammalian species we observed variation particularly within layer 6, and across ferret cortical areas we observed differences in expression patterns of upper layer markers. Our results provide molecular evidence that cortical layers 2/3, 4, 5 and 6 contain heterogeneous populations of molecularly defined neuronal subtypes that often segregate into sublayers, and that the molecular composition of these sublayers is largely conserved across mammalian superorders. Here we discuss the potential connectional and functional implications of these molecular and anatomical results.

Molecular markers identify sublaminations in the cell-rich layers

Carnivores have a relatively complex and well-studied visual system, and layer 4 of cat visual cortex is divided into two sublamina based on cytoarchitectonic and connectivity studies. Layer 4a contains larger, more widely separated neurons that receive substantial input from Y-cells of the lateral geniculate nucleus, and layer 4b contains smaller, densely packed neurons that are targeted by X-cells (Humphrey et al., 1985; Lund et al., 1979; O'Leary, 1941). One attractive possibility is that the molecular sublamination of layer 4 in ferret visual cortex (Fig. 4) correlates with neurons differentially receiving X and Y inputs. If so, we predict a similar gene expression pattern to be present in the cat. An even more complex pattern might be present in primate visual cortex, where layer 4 can be subdivided

into four sublamina, each with specific cytoarchitectonics and connectivity (Lund, 1988). Rodents are thought to have a less complex visual cortex and, in accord with this view, we were unable to detect a molecular sublamination to layer 4 in mouse visual cortex (Fig. 4).

Stratification of layer 5 has long been recognized by cytoarchitectonics and connectivity (Jones and Wise, 1977; Larkman and Mason, 1990; Lorente de No, 1943; Lund et al., 1979; Molnar and Cheung, 2006; O'Leary, 1941; Ramon y Cajal, 1899–1904; Thomson and Bannister, 2003). Lorente de No subdivided layer 5 into layers 5a, 5b, and 5c, with layer 5b containing the largest pyramidal neurons (Lorente de No, 1943). Modern authors typically only recognize a layer 5a and 5b, but some place the layer 5a – layer 5b boundary above the large pyramidal cells (Jones and Wise, 1977; Lund et al., 1979), while others place it below these cells (Larkman and Mason, 1990; Molnar and Cheung, 2006; Thomson and Bannister, 2003). Our molecular data securely identify a molecular layer 5 sublamination where layer 5b consists of the lower two-thirds of layer 5 and includes the large pyramidal cells (Fig. 5,6,10).

In carnivores, primates and rodents large pyramidal neurons near the top of layer 5b project subcortically to the brainstem and spinal cord (Gilbert and Kelly, 1975; Jones and Wise, 1977; Lund et al., 1979; Wise and Jones, 1977). In the mouse, it has been shown that the zinc-finger transcription factor *Fezf2* is expressed in these neurons, and genetic studies have demonstrated that *Fezf2* is involved in their development (Arlotta et al., 2004; Chen et al., 2005; Kwan et al., 2008; Molyneaux et al., 2005). We found that *FEZF2/Fezf2*, as well as two ion channel genes, *CACNA1H/Cacna1h* and *KCNN2/Kenn2*, identify layer 5b in ferret and mouse, indicating a conserved molecular sublamination to mammalian layer 5. Our results suggest that *FEZF2* and the two ion channel genes identify subcortically projecting neurons: the *FEZF2/CACNA1H/KCNN2*-positive neurons were particularly enriched in layer 5b of motor cortex, and many of these neurons had remarkably large cell bodies. These results suggest that molecular markers of key projection cell types, including corticospinal and corticotectal neurons, are conserved across mammals.

In mouse and ferret we observed a similar, but not identical, molecular sublamination to layer 6 (Fig. 7). This conserved molecular sublamination correlates with an established cytoarchitectonic subdivision of layer 6 into layer 6a and 6b (O'Leary, 1941; Peters and Yilmaz, 1993). Studies in primates and rodents suggest that upper and lower layer 6 differ in their efferent projections (Friedlander and Torres-Reveron, 2009; Gilbert and Kelly, 1975; Killackey and Sherman, 2003; LeVay and Sherk, 1981; Lund et al., 1975; Zhang and Deschenes, 1997). One specific possibility worth exploring in combination ISH and tracing experiments is that layers 6a and 6b target distinct thalamic nuclei (Killackey and Sherman, 2003; Zhang and Deschenes, 1997). In ferret and mouse there may be additional molecularly defined stratifications to layer 6 (see Fig. 10). For example, *EAG2* gene expression in ferret shows a gradient in layer 6a, potentially distinguishing an upper and lower layer 6a. It is possible that some of the connectional studies cited above reflect an upper and lower layer 6a subdivision, while others may follow the layer 6a/6b sublamination.

A cytoarchitectonic boundary between layer 2 and layer 3 has proved problematic for many authors (Bureau et al., 2006; Lorente de No, 1943; Lund, 1973; O'Leary, 1941). In cat, the size and packing density of pyramidal neurons increases in a graded manner within layers 2 and 3 (O'Leary, 1941). In ferret, we found that *SERPINE2* and *MDGA1* gene expression identified neurons at the top of layer 2/3, establishing that molecularly defined neuronal subtypes differentially populate these layers, and that these subtypes are organized into sublamina. In mouse barrel cortex, layer 2 has been distinguished from layer 3 as receiving paralemniscal input from the thalamus (Bureau et al., 2006), and our molecular subdivision of layer 2/3 may correlate with a similar connectional sublamination in the ferret.

Layer 4 markers and agranular cortical areas

Von Economo (1929) distinguished five fundamental types of neocortex according to the relative prominence of pyramidal cells and non-pyramidal “granular” cells within the cortical layers. In this scheme, agranular (type 1) cortex was identified in several territories, including motor, anterior cingulate and retrosplenial cortex (Rose and Woolsey, 1948). We found with the layer 4 markers *EAG2* and *RORB* clear molecular variability across these agranular areas (Fig. 4, 9), indicating that the molecular character of layer 4 is variable across classic agranular areas, although in a manner not predicted in previous classification schemes. Importantly, however, all the agranular areas examined expressed at least one layer 4 molecular marker. This observation suggests that agranular cortices have a functional layer 4, but that processing within layer 4 may be fundamentally different among motor cortex and the agranular medial limbic cortices.

Agranular motor cortex expressed both layer 4 markers *EAG2* and *RORB*. A transient cytoarchitectonic layer 4 has been identified early in development in the primary motor cortex of human and macaque monkey brains (Amunts et al., 1995; Brodmann, 1909; Huntley and Jones, 1991; Marin-Padilla, 1970). Our gene expression evidence in primary ferret motor cortex indicates the persistence of layer 4 cell types defined molecularly in the adult brain. It is likely that the *EAG2*+/*RORB*+ cells we observed in the motor cortex represent the target of input from the VL nucleus of the thalamus, as described in primate, carnivore and rodent brains (Kuramoto et al., 2009; Sloper and Powell, 1979; Strick and Sterling, 1974).

Conclusions

Our results establish molecular markers as a powerful complement to cytoarchitectonics and connection studies for layer and neuronal cell type definition. In the ferret cortex, we identified molecular markers for the cell-rich layers, and also identified molecular sublaminae to layers 2/3, 4, 5 and 6. In addition, we found that in both species the only consistently sharp boundary in gene expression within the cell-rich layers was between layers 4 and 5, confirming a prediction of Lorente de No (1943). This supports the notion that the cell-rich layers can be divided broadly into two major territories: the upper layers 2 – 4, and the deep layers 5 and 6. Upper layer marker expression varied more across cortical areas within species than in homologous areas between species. By contrast, deep layer gene expression remained constant across ferret cortical areas, but in layer 6 varied substantially across species. Despite this divergence, the organization of layer 6 into a 6a and 6b appears conserved.

Our data provide insight into the evolutionary constancy of the neocortical layers across mammals. The striking similarities in layer marker expression patterns support the notion that the neocortical layers and sublayers are evolutionarily stable, and are present in their essentials across all mammals. The ferret, as a representative carnivore, is currently thought to be an outgroup to both primates and rodents (Lindblad-Toh, 2004). As such, similarities in expression patterns between ferret and mouse should hold in primates too, including humans.

Supplementary Material

Refer to Web version on PubMed Central for supplementary material.

Acknowledgments

We thank Christine Labno and Vytas Bindokas of the University of Chicago IDDRC microscope facility, the University of Chicago ARC veterinary staff, Rahul Parnaik who developed the multi-color fluorescence ISH technique, and Elizabeth Grove, Ray Guillery and Murray Sherman who read the manuscript.

Grant Information

Grant sponsor: National Institutes of Health; Grant number: R01 EY016838.

LITERATURE CITED

- Allendoerfer K, Shatz C. The subplate, a transient neocortical structure: its role in the development of connections between thalamus and cortex. *Annu Rev Neurosci.* 1994; 17:185–218. [PubMed: 8210173]
- Amunts K, Istomin V, Schleicher A, Zilles K. Postnatal development of the human primary motor cortex: a quantitative cytoarchitectonic analysis. *Anat Embryol.* 1995; 192:557–571. [PubMed: 8751113]
- Arlotta P, Molyneaux BJ, Chen J, Inoue J, Kominami R, Macklis JD. Neuronal subtype-specific genes that control corticospinal motor neuron development in vivo. *Neuron.* 2004; 45:207–221. [PubMed: 15664173]
- Bannister AP. Inter- and intra-laminar connections of pyramidal cells in the neocortex. *Neuroscience Research.* 2005; 53:95–103. [PubMed: 16054257]
- Bizley JK, Nodal FR, Nelken I, King AJ. Functional organization of ferret auditory cortex. *Cereb Cortex.* 2005; 15:1637–1653. [PubMed: 15703254]
- Brodmann, K. *Lokalisationslehre der groshirnrinde in ihren principen dargestellt aus grund des zellenbaue.* Garey, L.J., translator. Leipzig: World Scientific Publishing Co; 1909. Barth. Translated by, 2006
- Bulfone A, Caccioppoli C, Pardini C, Faedo A, Martinez S, Banfi S. Pcp411, a novel gene encoding a Pcp4-like polypeptide, is expressed in specific domains of the developing brain. *Gene Expression Patterns.* 2004; 4:297–301. [PubMed: 15053978]
- Bureau I, von Saint Paul F, Svoboda K. Interdigitated paralemniscal and lemniscal pathways in the mouse barrel cortex. *PLoS Biol.* 2006; 4:e382. [PubMed: 17121453]
- Callaway EM, Lieber JL. Development of axonal arbors of layer 6 pyramidal neurons in ferret primary visual cortex. *J Comp Neurol.* 1996; 376:295–305. [PubMed: 8951644]
- Chen B, Schaevitz L, McConnell SK. Fezl regulates the differentiation and axon targeting of layer 5 subcortical projection neurons in cerebral cortex. *Proc Natl Acad Sci U S A.* 2005; 22:17184–17189. [PubMed: 16284245]
- Crowley JC, Katz LC. Early development of ocular dominance columns. *Science.* 2000; 290:1321–1324. [PubMed: 11082053]
- Feldblum S, Erlander MG, Tobin AJ. Different distributions of GAD65 and GAD67 mRNAs suggest that the two glutamate decarboxylases play distinctive functional roles. *J Neurosci Res.* 1993; 34:689–706. [PubMed: 8315667]
- Ferster D, LeVay S. The axonal arborizations of lateral geniculate neurons in the striate cortex of the cat. *J Comp Neurol.* 1978; 182:923–944. [PubMed: 103938]
- Frantz GD, McConnell SK. Restriction of late cerebral cortical progenitors to an upper-layer fate. 1996; 17:55–61.
- Fremeau RT, Troyer MD, Pahner I, Nygaard GO, Tran CH, Reimer RJ, Bellocchio EE, Fortin D, Storm-Mathisen J, Edwards RH. The expression of vesicular glutamate transporters defines two classes of excitatory synapse. *Neuron.* 2001; 31:247–260. [PubMed: 11502256]
- Friedlander M, Torres-Reveron J. The changing roles of neurons in the cortical subplate. *Front Neuroanat.* 2009; 3 Epub.
- Gabbott P, Somogyi P. Quantitative distribution of GABA-immunoreactive neurons in the visual cortex (area 17) of the cat. *Exp Brain Res.* 1986; 61:323–331. [PubMed: 3005016]

- Gilbert CD. Laminar differences in receptive field properties of cells in cat primary visual cortex. *J Physiol.* 1977; 268:391–421.
- Gilbert CD, Kelly JP. The projections of cells in different layers of the cat's visual cortex. *J Comp Neurol.* 1975; 163:81–106. [PubMed: 1159112]
- Gilbert CD, Wiesel TN. Intrinsic connectivity and receptive field properties in visual cortex. *Vis Res.* 1985; 25:365–374. [PubMed: 3895724]
- Goloboff P, Catalano S, Mirande J, Szumik C, Arias J, Kallersjo M, Farris J. Phylogenetic analysis of 73060 taxa corroborates major eukaryotic groups. *Cladistics.* 2009; 25:211–230.
- Grove EA, Tole S, Limon J, Yip L, Ragsdale CW. The hem of the embryonic cerebral cortex is defined by the expression of multiple Wnt genes and is compromised in Gli3-deficient mice. *Development.* 1998; 125:2315–2325. [PubMed: 9584130]
- Herculano-Houzel S, Collins CE, Wong P, Kaas JH, Lent R. The basic nonuniformity of the cerebral cortex. *Proc Natl Acad Sci U S A.* 2008; 105:12593–12598. [PubMed: 18689685]
- Heuer H, Christ S, Friedrichsen S, Brauer D, Winckler M, Bauer K, Raivich G. Connective tissue growth factor: a novel marker of layer VII neurons in the rat cerebral cortex. *Neuroscience.* 2003; 119:43–52. [PubMed: 12763067]
- Hevner RF. Layer-specific markers as probes for neuron type identity in human neocortex and malformations of cortical development. *Journal of Neuropathology & Experimental Neurology.* 2007; 66:101–109. [PubMed: 17278994]
- Hevner RF, Daza R, Rubenstein J, Stunnenberg H, Olavarria J, Englund C. Beyond laminar fate: toward a molecular classification of cortical projection/pyramidal neurons. *Dev Neurosci.* 2003; 25:139–151. [PubMed: 12966212]
- Higo S, Udaka N, Tamamaki N. Long-range GABAergic projection neurons in the cat neocortex. *J Comp Neurol.* 2007; 503:421. [PubMed: 17503478]
- Hoffman PN, Cleveland DW, Griffin JW, Landes PW, Cowan NJ, Price DL. Neurofilament gene expression: A major determinant of axonal caliber. *Proc Natl Acad Sci U S A.* 1987; 84:3472–3476. [PubMed: 3472217]
- Humphrey A, Sur M, Uhlrich D, Sherman S. Projection patterns of individual X- and Y-cell axons from the lateral geniculate nucleus to cortical area 17 in the cat. *J Comp Neurol.* 1985; 233:159–189. [PubMed: 3973100]
- Huntley G, Jones E. The emergence of architectonic field structure and areal borders in developing monkey sensorimotor cortex. *Neuroscience.* 1991; 44:287–310. [PubMed: 1719447]
- Hutsler JJ, Lee D-G, Porter KK. Comparative analysis of cortical layering and supragranular layer enlargement in rodent carnivore and primate species. *Brain Research.* 2005; 1052:71–81. [PubMed: 16018988]
- Inoue K, Terashima T, Nishikawa T, Takumi T. Fez1 is layer-specifically expressed in the adult mouse neocortex. *European Journal of Neuroscience.* 2004; 20:2909–2916. [PubMed: 15579145]
- Jones E, Wise S. Size, laminar and columnar distribution of efferent cells in the sensory-motor cortex of monkeys. *J Comp Neurol.* 1977; 175:391–438. [PubMed: 410849]
- Killackey H, Sherman SM. Corticothalamic projections from the rat primary somatosensory cortex. *J Neurosci.* 2003; 23:7381–7384. [PubMed: 12917373]
- Kirkcaldie MTK, Dickson TC, King CE, Grasby D, Riederer BM, Vickers JC. Neurofilament triplet proteins are restricted to a subset of neurons in the rat neocortex. *Journal of Chemical Neuroanatomy.* 2002; 24:163–171. [PubMed: 12297262]
- Krettek J, Price J. Projections from the amygdaloid complex to the cerebral cortex and thalamus in the rat and cat. *J Comp Neurol.* 1977; 172:687–722. [PubMed: 838895]
- Kuramoto E, Furuta T, Nakamura KC, Unzai T, Hioki H, Kaneko T. Two types of thalamocortical projections from the motor thalamic nuclei of the rat: a single neuron-tracing study using viral vectors. *Cereb Cortex.* 2009; 19:2065–2077. [PubMed: 19174446]
- Kwan K, Lam M, Krsnik Z, Kawasaki Y, Lefebvre V, Sestan N. SOX5 postmitotically regulates migration, postmigratory differentiation, and projections of subplate and deep-layer neocortical neurons. *Proc Natl Acad Sci U S A.* 2008; 105:16021–16026. [PubMed: 18840685]

- Larkman A, Mason A. Correlations between morphology and electrophysiology of pyramidal neurons in slices of rat visual cortex. I. Establishment of cell classes. *J Neurosci.* 1990; 10:1407–1414. [PubMed: 2332787]
- Law MI, Zahs KR, Stryker MP. Organization of primary visual cortex (area 17) in the ferret. *J Comp Neurol.* 1988; 278:157–180. [PubMed: 3068264]
- Lein ES, Hawrylycz MJ, Ao N, Ayres M, Bensinger A, Bernard A, Boe AF, Boguski MS, Brockway KS, Byrnes EJ, Chen L, Chen L, Chen T-M, Chi Chin M, Chong J, Crook BE, Czaplinska A, Dang CN, Datta S, Dee NR, Desaki AL, Desta T, Diep E, Dolbeare TA, Donelan MJ, Dong H-W, Dougherty JG, Duncan BJ, Ebbert AJ, Eichele G, Estin LK, Faber C, Facer BA, Fields R, Fischer SR, Fliss TP, Frensley C, Gates SN, Glattfelder KJ, Halverson KR, Hart MR, Hohmann JG, Howell MP, Jeung DP, Johnson RA, Karr PT, Kawal R, Kidney JM, Knapik RH, Kuan CL, Lake JH, Laramee AR, Larsen KD, Lau C, Lemon TA, Liang AJ, Liu Y, Luong LT, Michaels J, Morgan JJ, Morgan RJ, Mortrud MT, Mosqueda NF, Ng LL, Ng R, Orta GJ, Overly CC, Pak TH, Parry SE, Pathak SD, Pearson OC, Puchalski RB, Riley ZL, Rockett HR, Rowland SA, Royall JJ, Ruiz MJ, Sarno NR, Schaffnit K, Shapovalova NV, Sivisay T, Slaughterbeck CR, Smith SC, Smith KA, Smith BI, Sodd AJ, Stewart NN, Stumpf K-R, Sunkin SM, Sutram M, Tam A, Teemer CD, Thaller C, Thompson CL, Varnam LR, Visel A, Whitlock RM, Wohnoutka PE, Wolkey CK, Wong VY, Wood M, Yaylaoglu MB, Young RC, Youngstrom BL, Feng Yuan X, Zhang B, Zwingman TA, Jones AR. Genome-wide atlas of gene expression in the adult mouse brain. *Nature.* 2007; 445:168–176. [PubMed: 17151600]
- Leone DP, Srinivasan K, Chen B, Alcamo E, McConnell SK. The determination of projection neuron identity in the developing cerebral cortex. *Current Opinion in Neurobiology.* 2008; 18:28–35. [PubMed: 18508260]
- LeVay S, Gilbert CD. Laminar patterns of geniculocortical projections in the cat. *Brain Research.* 1976; 113:1–19. [PubMed: 953720]
- LeVay S, Sherk H. The visual claustrum of the cat. I. Structure and connections. *J Neurosci.* 1981; 1:956–980. [PubMed: 6169810]
- Lewis WB. Researches on the comparative structure of the cortex cerebri. *Philosophical Transactions of the Royal Society of London.* 1880; 171:35–64.
- Lewis WB. On the comparative structure of the brain in rodents. *Philosophical Transactions of the Royal Society of London.* 1882; 173:699–794.
- Lewis WB, Clarke H. The cortical lamination of the motor area of the brain. *Proceedings of the Royal Society of London.* 1878; 27:38–49.
- Lindblad-Toh K. Genome sequencing: three's company. *Nature.* 2004; 428:475–476. [PubMed: 15057812]
- Lorente de No, R. Cerebral cortex: architecture, intracortical connections, motor projections. In: Fulton, JF., editor. *Physiology of the nervous system.* London: Oxford University Press; 1943. p. 274-298.
- Ludwig J, Weseloh R, Karschin C, Liu Q, Netzer R, Engeland B, Stansfeld C, Pongs O. Cloning and functional expression of rat eag2, a new member of the ether-a-go-go family of potassium channels and comparison of its distribution with that of eag1. *Molecular and Cellular Neuroscience.* 2000; 16:59–70. [PubMed: 10882483]
- Lund J. Organisation of neurons in the visual cortex, area 17, of the monkey (*Macaca mulatta*). *J Comp Neurol.* 1973; 147:455–496. [PubMed: 4122705]
- Lund J. Anatomical organization of macaque monkey striate visual cortex. *Annu Rev Neurosci.* 1988; 11:253–288. [PubMed: 3284442]
- Lund J, Henry G, Macqueen C, Harvey A. Anatomical organization of the primary visual cortex (area 17) of the cat. A comparison with area 17 of the macaque monkey. *J Comp Neurol.* 1979; 184:599–618. [PubMed: 106072]
- Lund J, Lund R, Hendrickson A, Bunt A, Fuchs A. The origin of efferent pathways from the primary visual cortex, area 17, of the macaque monkey as shown by retrograde transport of horseradish peroxidase. *J Comp Neurol.* 1975; 164:287–304. [PubMed: 810501]
- Lunter G. Dog as an outgroup to human and mouse. *PLoS Comput Biol.* 2007; 3:e74. [PubMed: 17465673]

- Madsen O, Scally M, Douady CJ, Kao DJ, DeBry RW, Adkins R, Amrine HM, Stanhope MJ, de Jong WW, Springer MS. Parallel adaptive radiations in two major clades of placental mammals. *Nature*. 2001; 409:610–614. [PubMed: 11214318]
- Manger PR, Kiper D, Masiello I, Murillo L, Tettoni L, Hunyadi Z, Innocenti GM. The representation of the visual field in three extrastriate areas of the ferret (*Mustela putorius*) and the relationship of retinotopy and field boundaries to callosal connectivity. *Cereb Cortex*. 2002; 12:423–437. [PubMed: 11884357]
- Marin-Padilla M. Prenatal and early postnatal ontogenesis of the human motor cortex: a Golgi study. I. The sequential development of the cortical layers. *Brain Res*. 1970; 23:167–183. [PubMed: 4097697]
- Masland RH. Neuronal cell types. *Current Biology*. 2004; 14:R497–R500. [PubMed: 15242626]
- Meynert, T. The brain of mammals. In: Stricker, S., editor. *Manual of Human and Comparative Histology*. London: The New Sydenham Society; 1872. p. 367-411.
- Molnar Z, Cheung AFP. Towards the classification of subpopulations of layer V pyramidal projection neurons. *Neuroscience Research*. 2006; 55:105–115. [PubMed: 16542744]
- Molyneaux BJ, Arlotta P, Hirata T, Hibi M, Macklis JD. Fezl is required for the birth and specification of corticospinal motor neurons. 2005; 47:817–831.
- Molyneaux BJ, Arlotta P, MacDonald J, MacQuarrie K, Macklis JD. Novel subtype-specific genes identify distinct subpopulations of callosal projection neurons. *J Neurosci*. 2009; 29:12343–12354. [PubMed: 19793993]
- Molyneaux BJ, Arlotta P, Menezes JRL, Macklis JD. Neuronal subtype specification in the cerebral cortex. *Nat Rev Neurosci*. 2007; 8:427–437. [PubMed: 17514196]
- Murphy WJ, Eizirik E, Johnson WE, Zhang YP, Ryder OA, O'Brien SJ. Molecular phylogenetics and the origins of placental mammals. *Nature*. 2001; 6820:614–618. [PubMed: 11214319]
- Nagamine S, Koike S, Keino-Masu K, Masu M. Expression of a heparan sulfate remodeling enzyme, heparan sulfate 6-O-endosulfatase sulfatase FP2, in the rat nervous system. *Developmental Brain Research*. 2005; 159:135–143. [PubMed: 16139897]
- Nelson SB, Sugino K, Hempel CM. The problem of neuronal cell types: a physiological genomics approach. *Trends in Neurosciences*. 2006; 29:339–345. [PubMed: 16714064]
- Ng L, Bernard A, Lau C, Overly CC, Dong H-W, Kuan C, Pathak S, Sunkin SM, Dang C, Bohland JW, Bokil H, Mitra PP, Puelles L, Hohmann J, Anderson DJ, Lein ES, Jones AR, Hawrylycz M. An anatomic gene expression atlas of the adult mouse brain. *Nat Neurosci*. 2009; 12:356–362. [PubMed: 19219037]
- Ng L, Lau C, Sunkin SM, Bernard A, Chakravarty M, Lein ES, Jones AR, Hawrylycz M. Surface-based mapping of gene expression and probabilistic expression maps in the mouse cortex. *Methods*. 2010; 50:55–62. [PubMed: 19818854]
- Nieto M, Monuki ES, Tang H, Imitola J, Haubst N, Khoury SJ, Cunningham J, Gotz M, Walsh CA. Expression of Cux-1 and Cux-2 in the subventricular zone and upper layers II-IV of the cerebral cortex. *The Journal of Comparative Neurology*. 2004; 479:168–180. [PubMed: 15452856]
- Northcutt RG, Kaas JH. The emergence and evolution of mammalian neocortex. *Trends in Neurosciences*. 1995; 18:373–379. [PubMed: 7482801]
- O'Leary J. Structure of the area striate of the cat. *J Comp Neurol*. 1941; 75:131–161.
- Okano HJ, Darnell RB. A hierarchy of Hu RNA binding proteins in developing and adult neurons. *J Neurosci*. 1997; 17:3024–3037. [PubMed: 9096138]
- Pallas SL, Roe AW, Sur M. Visual projections induced into the auditory pathway of ferrets. I. Novel inputs to primary auditory cortex (AI) from the LP/pulvinar complex and the topography of the MGN-AI projection. *J Comp Neurol*. 1990; 298:50–68. [PubMed: 1698829]
- Peters A, Yilmaz E. Neuronal organization in area 17 of cat visual cortex. *Cereb Cortex*. 1993; 3:49–68. [PubMed: 7679939]
- Rakic P. Confusing cortical columns. *Proc Natl Acad Sci U S A*. 2008; 105:12099–12100. [PubMed: 18715998]
- Ramon y Cajal, S. *Textura del sistema nervioso del hombre y de los vertebrados. Estudios sobre el plan estructural y composición histológica de los centros nerviosos adicionados de consideraciones fisiológicas fundadas en los nuevos descubrimientos*. In: Moya, N., editor. Madrid: Oxford

- University Press; 1899–1904. Translated from the Spanish by L. Azoulay. Translated from the French by N. Swanson and L.W. Swanson, 1995
- Reinhard E, Suidan H, Pavlik A, Monard D. Glia-derived nexin/protease nexin-1 is expressed by a subset of neurons in the rat brain. *J Neurosci Res.* 1994; 37:256–270.
- Rockel AJ, Hiorns RW, Powell TPS. The basic uniformity in structure of the neocortex. *Brain.* 1980; 103:221–244. [PubMed: 6772266]
- Rockland KS. Anatomical organization of primary visual cortex (area 17) in the ferret. *J Comp Neurol.* 1985; 241:225–236. [PubMed: 4067016]
- Rockland KS, Ichinohe N. Some thoughts on cortical minicolumns. *Exp Brain Res.* 2004; 158:265–277. [PubMed: 15365664]
- Rose J, Woolsey C. Structure and relations of limbic cortex and anterior thalamic nuclei in rabbit and cat. *J Comp Neurol.* 1948; 89:279–347. [PubMed: 18103781]
- Saganich MJ, de Miera EV-S, Nadal MS, Baker H, Coetzee WA, Rudy B. Cloning of components of a novel subthreshold-activating K⁺ channel with a unique pattern of expression in the cerebral cortex. *J Neurosci.* 1999; 19:10789–10802. [PubMed: 10594062]
- Sailer CA, Hu H, Kaufmann WA, Trieb M, Schwarzer C, Storm JF, Knaus H-G. Regional differences in distribution and functional expression of small-conductance Ca²⁺-activated K⁺ channels in rat brain. *J Neurosci.* 2002; 22:9698–9707. [PubMed: 12427825]
- Schaeren-Wiemers N, Andre E, Kapfhammer JP, Becker-Andre M. The expression pattern of the orphan nuclear receptor RORbeta in the developing and adult rat nervous system suggests a role in the processing of sensory information and in circadian rhythm. *Eur J Neurosci.* 1997; 9:2687–2701. [PubMed: 9517474]
- Shu W, Yang H, Zhang L, Lu MM, Morrisey EE. Characterization of a new subfamily of winged-helix/forkhead (Fox) genes that are expressed in the lung and act as transcriptional repressors. *J Biol Chem.* 2001; 276:27488–27497. [PubMed: 11358962]
- Skoglund TS, Pascher R, Berthold CH. Heterogeneity in the columnar number of neurons in different neocortical areas in the rat. *Neuroscience Letters.* 1996; 208:97–100. [PubMed: 8859899]
- Sloper JJ, Powell TPS. An experimental electron microscopic study of afferent connections to the primate motor and somatic sensory cortices. *Philosophical Transactions of the Royal Society of London.* 1979; 285:199–226. [PubMed: 36639]
- Smart I, McSherry G. Gyrus formation in the cerebral cortex of the ferret. II. Description of the internal histological changes. *J Anat.* 1986; 147:27–43. [PubMed: 3693076]
- Strick P, Sterling P. Synaptic termination of afferents from the ventrolateral nucleus of the thalamus in the cat motor cortex. A light and electron microscopy study. *J Comp Neurol.* 1974; 153:77–106. [PubMed: 4817346]
- Symonds L, Rosenquist A. Laminal origins of visual corticocortical connections in the cat. *J Comp Neurol.* 1984; 229:39–47. [PubMed: 6490975]
- Takeuchi A, Hamasaki T, Litwack ED, O'Leary DDM. Novel IgCAM, MDGA1, expressed in unique cortical area- and layer-specific patterns and transiently by distinct forebrain populations of cajal-retzius neurons. *Cereb Cortex.* 2007; 17:1531–1541. [PubMed: 16959869]
- Talley EM, Cribbs LL, Lee J-H, Daud A, Perez-Reyes E, Bayliss DA. Differential distribution of three members of a gene family encoding low voltage-activated (T-type) calcium channels. *J Neurosci.* 1999; 19:1895–1911. [PubMed: 10066243]
- Tarabykin V, Stoykova A, Usman N, Gruss P. Cortical upper layer neurons derive from the subventricular zone as indicated by Svet1 gene expression. *Development.* 2001; 128:1983–1993. [PubMed: 11493521]
- Thomson AM, Bannister AP. Interlaminar connections in the neocortex. *Cereb Cortex.* 2003; 13:5–14. [PubMed: 12466210]
- Ullrich B, Sudhof TC. Differential distributions of novel synaptotagmins: Comparison to synapsins. *Neuropharmacology.* 1995; 34:1371–1377. [PubMed: 8606786]
- von Economo, C. The cytoarchitectonics of the human cerebral cortex. Parker, S., translator. London: Oxford University Press; 1929.
- Ware ML, Tavazoie SF, Reid CB, Walsh CA. Coexistence of widespread clones and large radial clones in early embryonic ferret cortex. *Cereb Cortex.* 1999; 9:636–645. [PubMed: 10498282]

- Watakabe A, Ichinohe N, Ohsawa S, Hashikawa T, Komatsu Y, Rockland KS, Yamamori T. Comparative analysis of layer-specific genes in mammalian neocortex. *Cereb Cortex*. 2007; 17:1918–1933. [PubMed: 17065549]
- Wise S, Jones E. Cells of origin and terminal distribution of descending projections of the rat somatic sensory cortex. *J Comp Neurol*. 1977; 175:129–158. [PubMed: 408380]
- Zhang Z-W, Deschenes M. Intracortical axonal projections of lamina VI cells of the primary somatosensory cortex in the rat: A single-cell labeling study. *J Neurosci*. 1997; 17:6365–6379. [PubMed: 9236245]

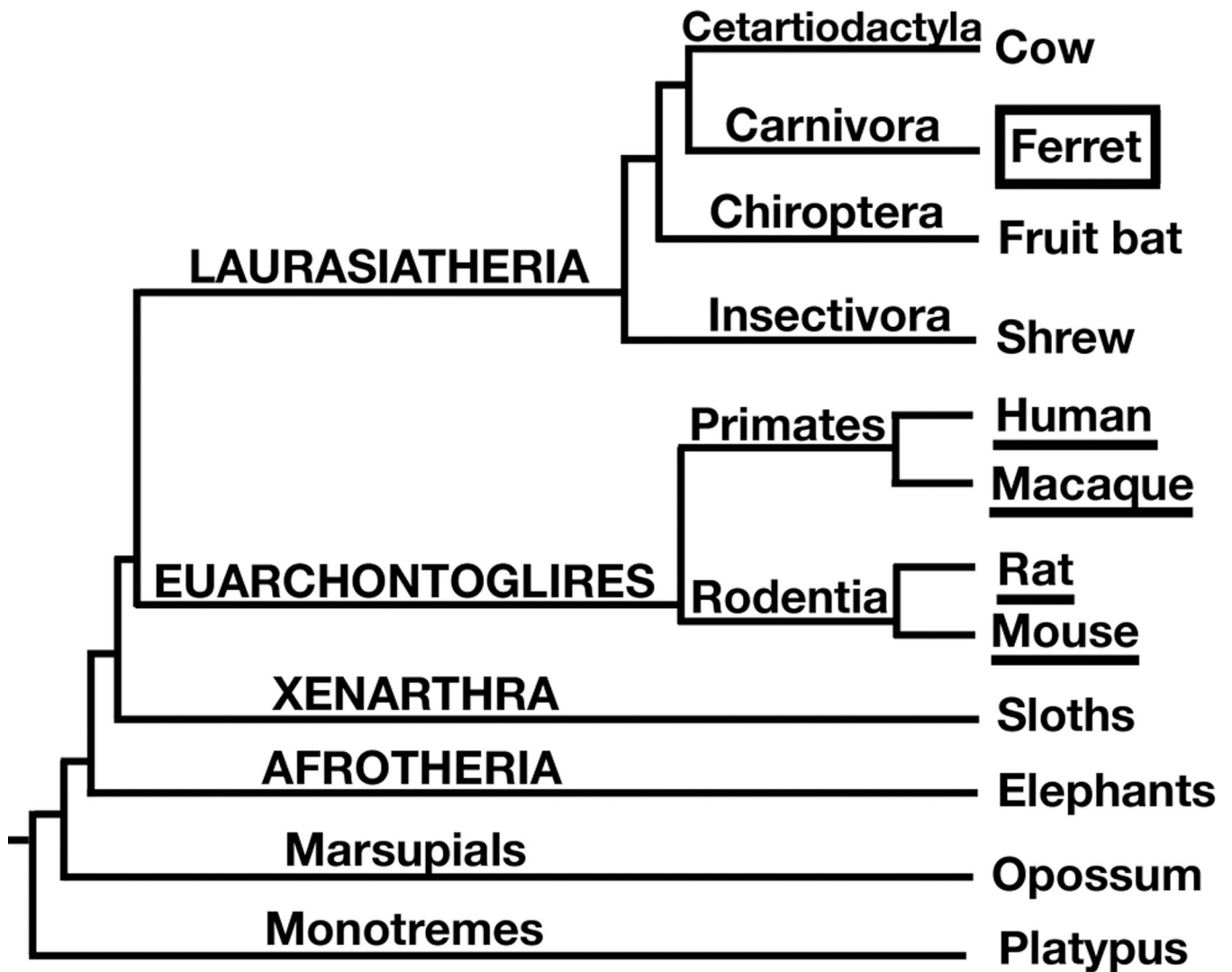


Figure 1. Phylogeny of living mammals

Layer marker gene expression patterns have previously been studied in rodents and primates (underlined), which are members of the superorder Euarchontoglires. The ferret and other carnivores (boxed) are members of the separate superorder, Laurasiatheria. Adapted from Lindblad-Toh, 2004.

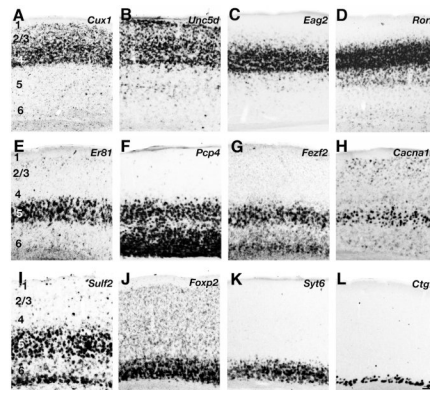


Figure 2. Layer marker gene expression in adult mouse visual cortex

Gene expression patterns of upper layer markers *Cux1* (A), *Unc5d* (B), *Eag2* (C) and *Rorb* (D), and deep layer markers *Er81* (E), *Pcp4* (F), *Fezf2* (G), *Cacna1h* (H), *Sulf2* (I), *Foxp2* (J), *Syt6* (K) and *Ctgf* (L) are depicted. Scale bar is 100 μ m.

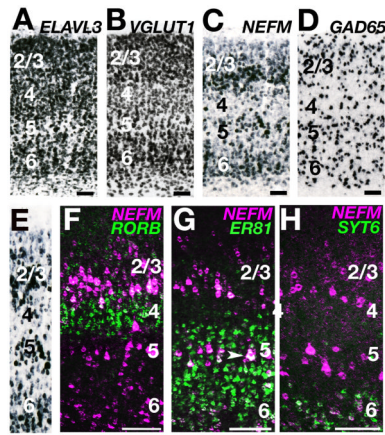


Figure 3. Ferret neocortical layers can be identified with pan-neuronal genes and ‘rodent’ layer markers

A – E: Expression patterns of *ELAVL3* (A), *VGLUT1* (B), *NEFM* (C, E) and *GAD65* (D) in adult ferret visual cortex. Panels A – C illustrate serially adjoining sections. **F – H:** Two color expression profiles of candidate layer markers (green) and *NEFM* (magenta) in adult ferret visual cortex. **F:** *RORB* (green) is expressed in layer 4 (gap in *NEFM* expression between layers 2/3 and 5). **G:** *ER81* (green) is expressed in layers 5 and 6 (the center of layer 5 contains the largest *NEFM* expressing cells, arrowhead). **H:** *SYT6* (green) is expressed in layer 6 (small, densely packed *NEFM* expressing cells below layer 5). Panels F, G, and H are photomicrograph pairs stitched together with Photoshop CS3 software. Scale bars are 100µm.

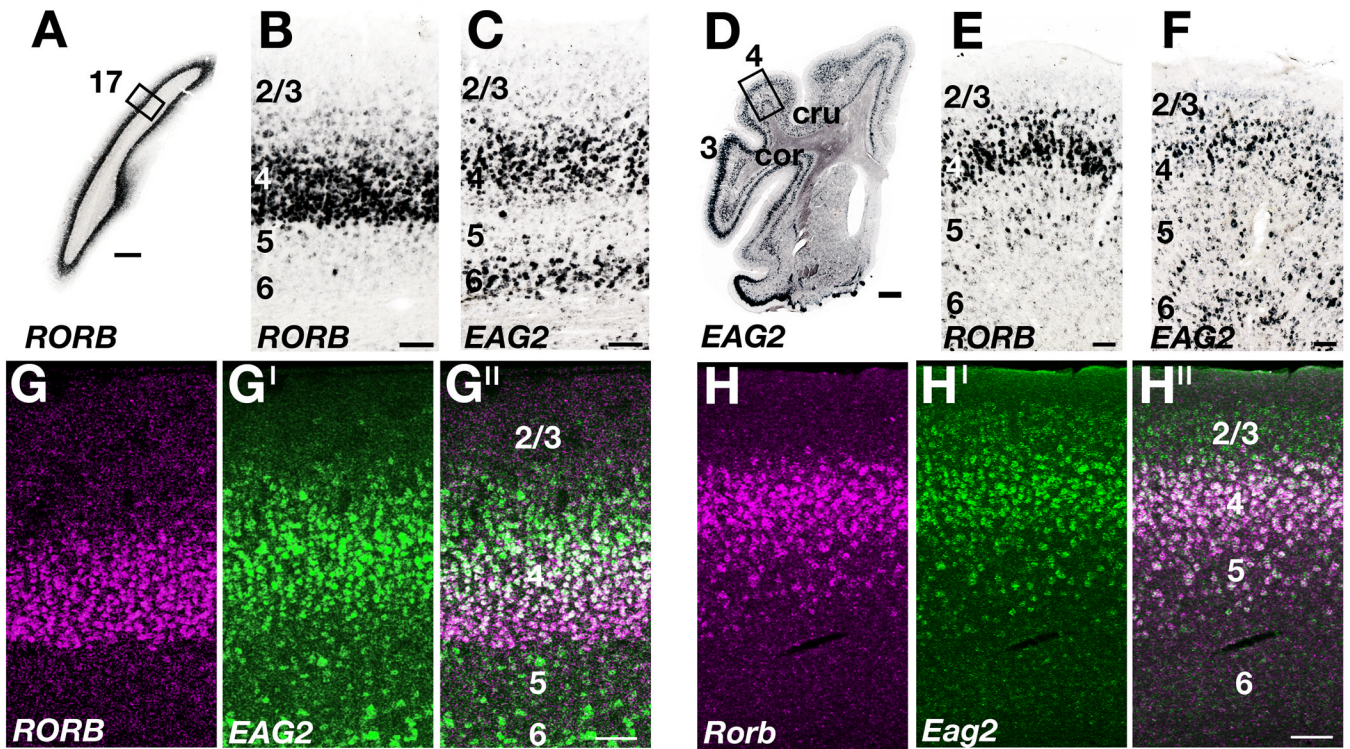


Figure 4. Layer 4 marker gene expression patterns in ferret and mouse neocortex
A – C: Expression patterns of *RORB* and *EAG2* in ferret primary visual cortex (area 17). *RORB* ISH labels layer 4 (A, B), whereas *EAG2* mRNA identifies layers 4 and 6 (C). **D – F:** Expression patterns of *RORB* and *EAG2* in ferret motor cortex (area 4). Similar to visual cortex, *RORB* mRNA is enriched in layer 4 (E), while *EAG2* is expressed in layers 4 and 6 (D, F). The width of *EAG2*+ layer 6 is expanded at the top of the coronal gyrus (F), reflecting the changes in the relative thickness of layers across smooth, gyral, and sulcal cortices (Brodmann, 1909; Smart and McSherry, 1986). **G – G'':** Two color expression profile of *RORB* (magenta in G, G') and *EAG2* (green in G', G'') in ferret visual cortex. **H – H'':** Two-color expression profile of *Rorb* (magenta in H, H'') and *Eag2* (green in H', H'') in mouse visual cortex. Sublamination of layer 4 is evident in ferret (G') but not mouse (H'') visual cortex. Panel D constructed from two images by Photoshop CS3. In panels A and D the scale bar is 1mm; in all other panels scales bar are 100 μ m. cru, cruciate sulcus; cor, coronal sulcus; 17, visual cortex; 4, motor cortex; 3, somatosensory cortex.

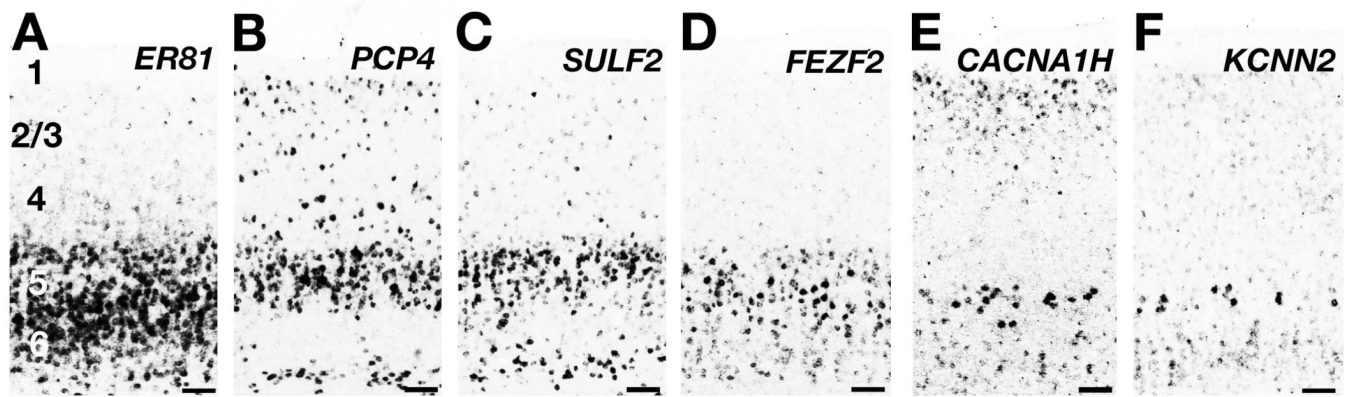


Figure 5. ‘Layer 5’ molecular markers are expressed in layers 5 and 6 of the ferret neocortex
A – F: Layer 5 marker expression patterns in adult ferret primary visual cortex (area 17). **A:** *ER81* is expressed throughout layers 5 and 6. **B, C:** *PCP4* (B) and *SULF2* (C) ISH labels neurons in layer 5 and deep layer 6. **D:** *FEZF2* is strongly expressed in deep layer 5 and weakly in upper layer 6. **E, F:** *CACNA1H* (E) and *KCNN2* (F) are expressed particularly strongly in the lower part of layer 5 and in upper layer 6. Scale bars are 100µm.

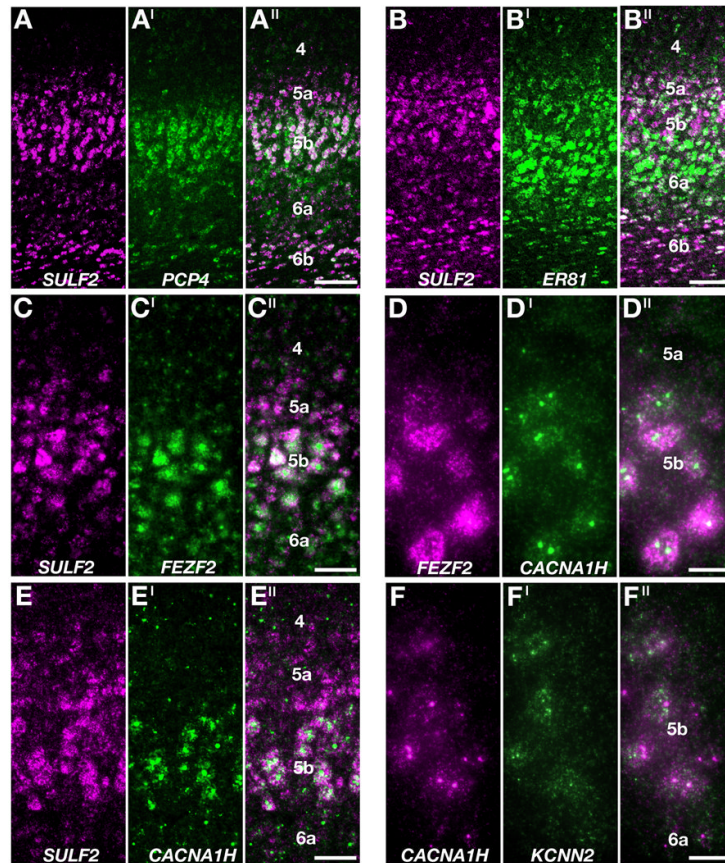


Figure 6. Molecular markers demonstrate layer 5 sublamination in ferret motor cortex
A – F'': Two color coexpression profiles in adult ferret motor cortex (area 4). **A – A''**: *SULF2* (magenta in A, A'') but not *PCP4* (green in A', A'') message labels layer 5a, but these genes are extensively coexpressed in layer 5b and deep layer 6. **B – B''**: Comparison of *SULF2* (magenta in B, B'') and *ER81* (green in B', B'') mRNA distributions demonstrates that *ER81* is expressed throughout layers 5 and 6. **C – C''**: *FEZF2* mRNA selectively labels neurons in layer 5b (green in C', C''), as demonstrated by comparison with *SULF2* expression (magenta in C, C''). **D – D''**: *FEZF2* (magenta in D, D'') and *CACNA1H* (green in D', D'') coexpression in layer 5b. **E – E''**: Comparison of *SULF2* (magenta in E, E'') and *CACNA1H* (green in E', E'') demonstrates that *CACNA1H* message is enriched in layer 5b. **F – F''**: *CACNA1H* (magenta in F, F'') and *KCNN2* (green in F', F'') coexpression in layer 5b. The mRNA of both genes localize as puncta within cell bodies. Scale bars in A'' (for A – A') and B'' (for B – B'') are 100 μ m, in C'' (for C – C') and D'' (for D – D') are 50 μ m, in E'' (for E – E') and F'' (for F – F') are 25 μ m.

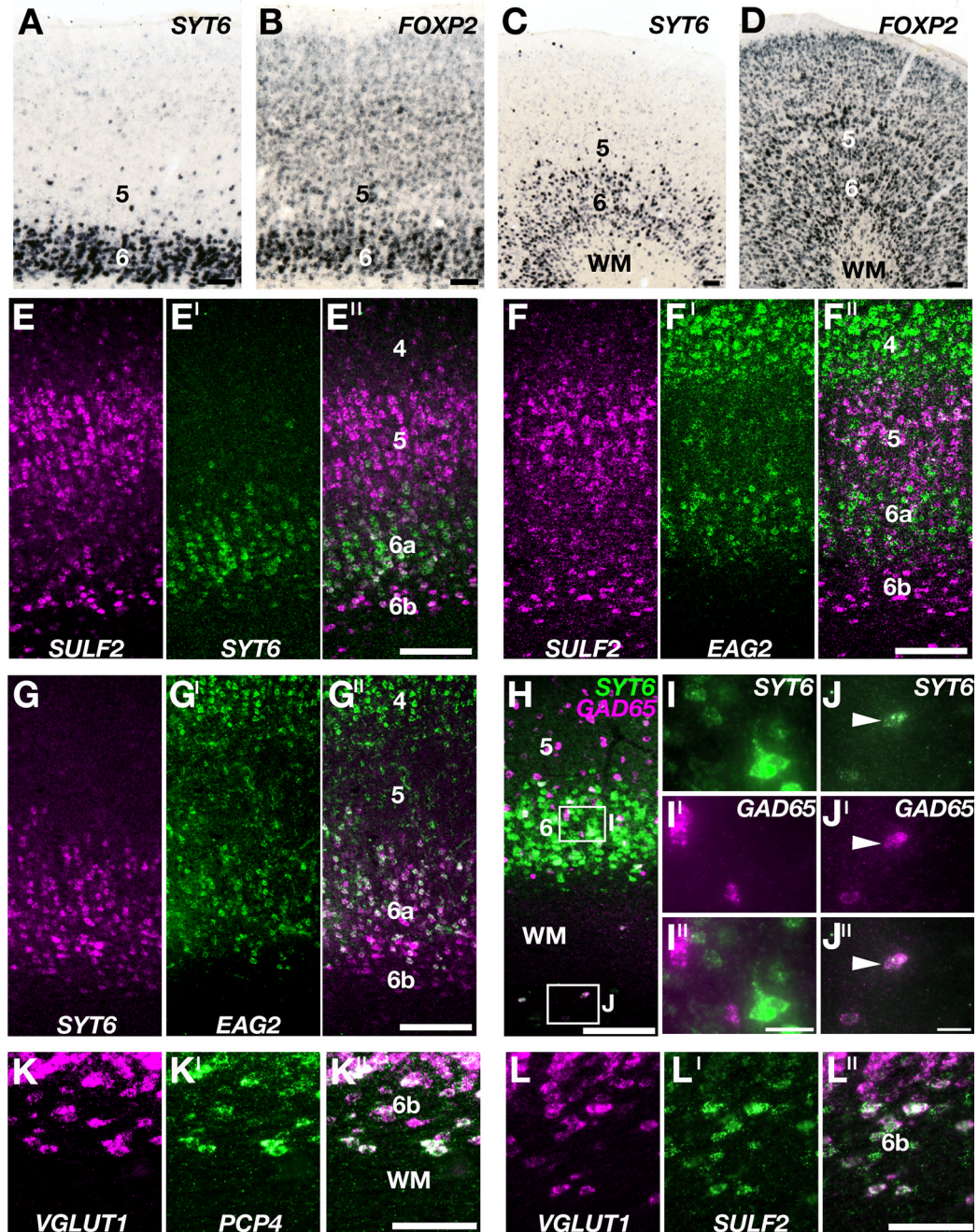


Figure 7. Molecular identification of a layer 6a and layer 6b in ferret cortex

A – D: Expression of *SYT6* (A,C) and *FOXP2* (B,D) in adult ferret visual cortex (A,B) and motor cortex (C,D). **A, C:** *SYT6* ISH selectively identifies cells in layer 6 across cortical areas. **B, D:** *FOXP2* expression is enhanced in layer 6 of visual cortex (B), but layer 6 selectivity is almost absent from motor cortex (D). **E – L'':** Two color gene expression profiles in ferret visual cortex (area 17). **E – F'':** Layer 6a is characterized by strong *SYT6* (green in E', E'') and *EAG2* (green in F', F'') gene expression, whereas neurons in layer 6b are enriched with *SULF2* mRNA (magenta in E, E'', F, F''). **G:** Comparing *EAG2* (green in G', G'') and *SYT6* (magenta in G, G'') expression demonstrates that *EAG2* message is enriched in the upper part of layer 6a, although scattered *EAG2*+ neurons are located

throughout layer 6a. **H**: *SYT6* (green) and *GAD65* (magenta) gene expression in layer 6a (Box I) and in the white matter (Box J). **I – I''**: Higher magnification of tissue in Box I. *SYT6* (green in I, I'') and *GAD65* (magenta in I', I'') are not coexpressed in layer 6a. **J – J''**: Higher magnification of Box J. Neurons enriched in *SYT6* mRNA (green in J, J''; arrowhead) in the white matter coexpress *GAD65* (magenta in J', J''; arrowhead). **K – L''**: *PCP4*- (green in K', K'') and *SULF2*- (green in L', L'') enriched neurons in layer 6b express the glutamatergic marker *VGLUT1* (magenta in panels K, K'', L, L''). Scale bars are 100µm. WM, white matter.

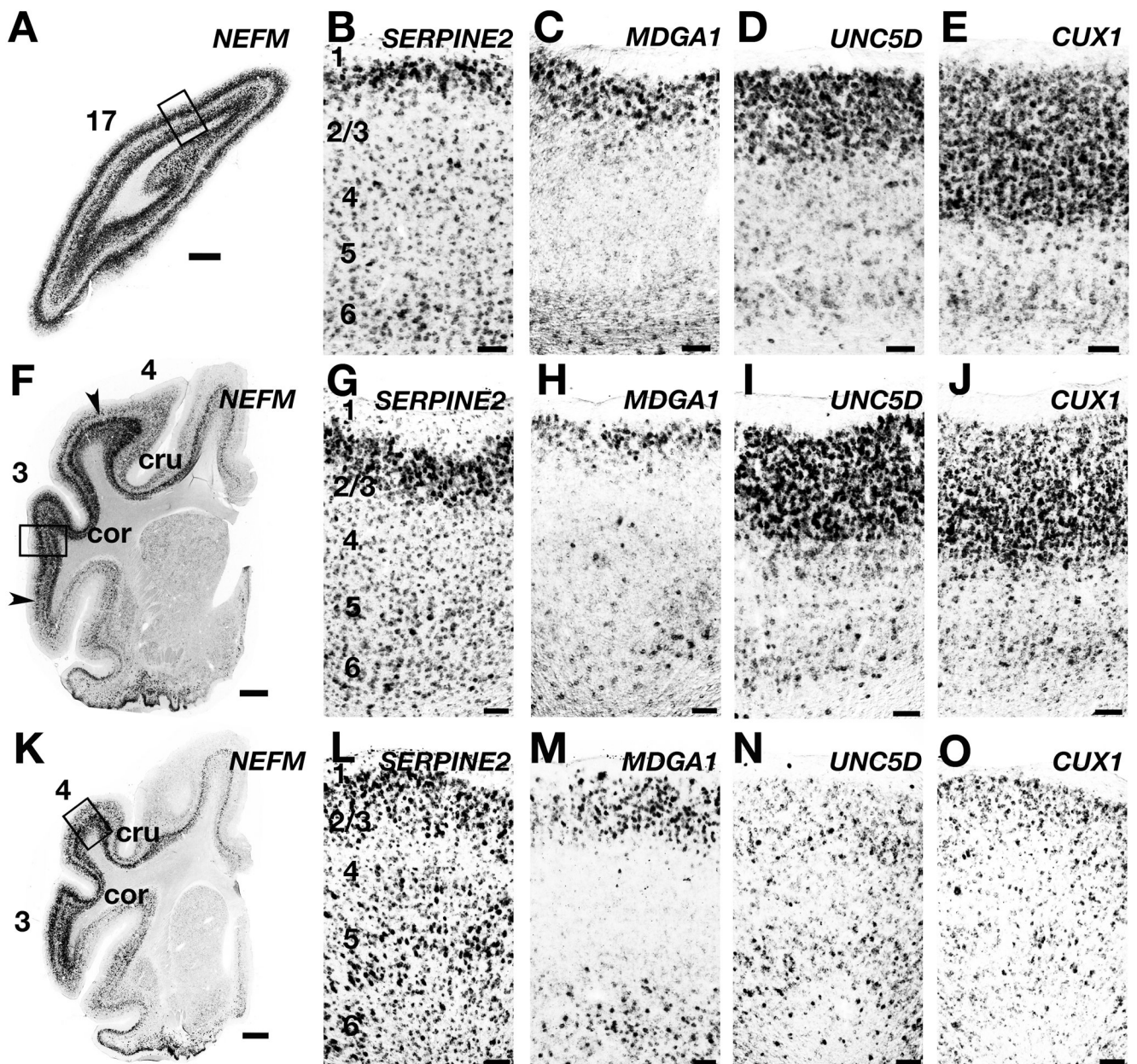


Figure 8. Upper layer marker gene expression patterns across ferret cortical areas

A – O: Expression of upper layer markers in primary visual (A – E), somatosensory (F – J), and motor (K – O) cortex. **A, F, K:** Low-power images of tissue probed for *NEFM* in visual (A) and somatomotor (F, K) areas. Boxes indicate the territory from which high-power images were taken. **B, G, L:** *SERPINE2* mRNA is dense in the superficial part of layer 2/3, with extensive expression in scattered cells throughout the cortical layers. **C, H, M:** *MDGA1* is expressed in the superficial part of layer 2/3, and is also enriched in layer 6, particularly in motor cortex (M). **D, I, N:** *UNC5D* is expressed strongly in the upper layers of visual (D) and somatosensory (I) cortex but not motor cortex (N). **E, J, O:** *CUX1* mRNA is enriched in the upper layers of visual (E) and somatosensory (J) cortex, but not motor (O) cortex. Scale bars in A, F, K are 1mm, and in all other panels are 100 μ m. cru, cruciate sulcus; cor, coronal sulcus; 17, visual cortex; 4, motor cortex; 3, somatosensory cortex.

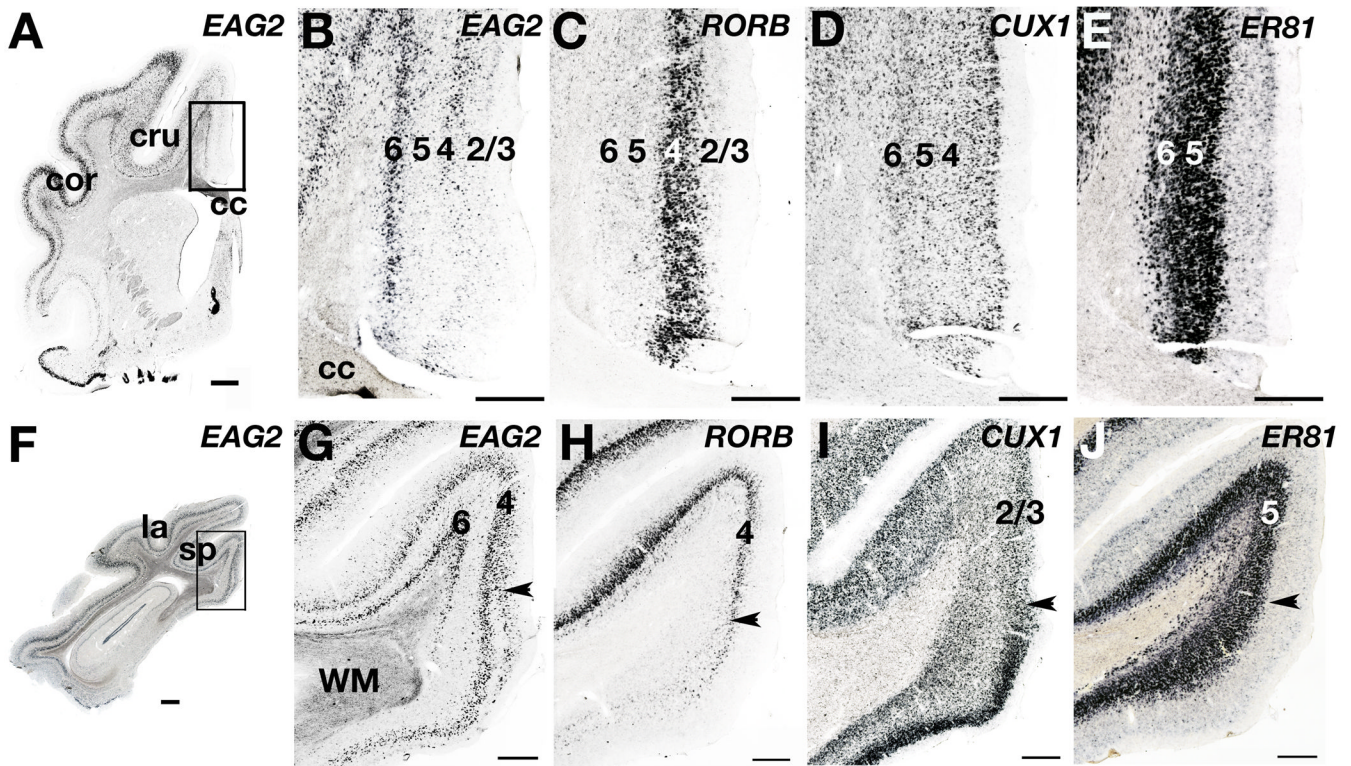


Figure 9. Ferret layer marker gene expression in the medial limbic cortex

A–E: Expression patterns in the anterior limbic cortex. **A:** *EAG2*-labeled tissue at low-power magnification, with the boxed area indicating the region photographed in panels **B – E**. **B – E:** In the agranular anterior limbic area *EAG2* expression in layer 4 is dramatically reduced (**B**) whereas *RORB* message enrichment in layer 4 is maintained (**C**). *CUX1* mRNA does not show enrichment in layers 2 – 4 (**D**), and *ER81* ISH labels layers 5 and 6 (**E**). **F – J:** Expression patterns in the posterior limbic cortex. **F:** *EAG2* expression with the box identifying the territory photographed in panels **G – J**. **G – J:** Arrowhead marks the transition between the posterior cingulate cortex (above arrowhead) and the retrosplenial cortex (below arrowhead). With the transition from posterior cingulate to retrosplenial cortex, *EAG2* expression in layer 4 splits into two bands (**G**), layer 4 *RORB* expression is lost (**H**), *CUX1* expression in the upper layers dramatically increases in density and intensity (**I**), but *ER81* mRNA maintains its expression pattern in layers 5 and 6. Scale bars are 1mm (**A,F**), or 100µm (**B – E, G – J**). cc, corpus callosum; cru, cruciate sulcus; cor, coronal sulcus; la, lateral sulcus; sp, splenial sulcus; WM, white matter.

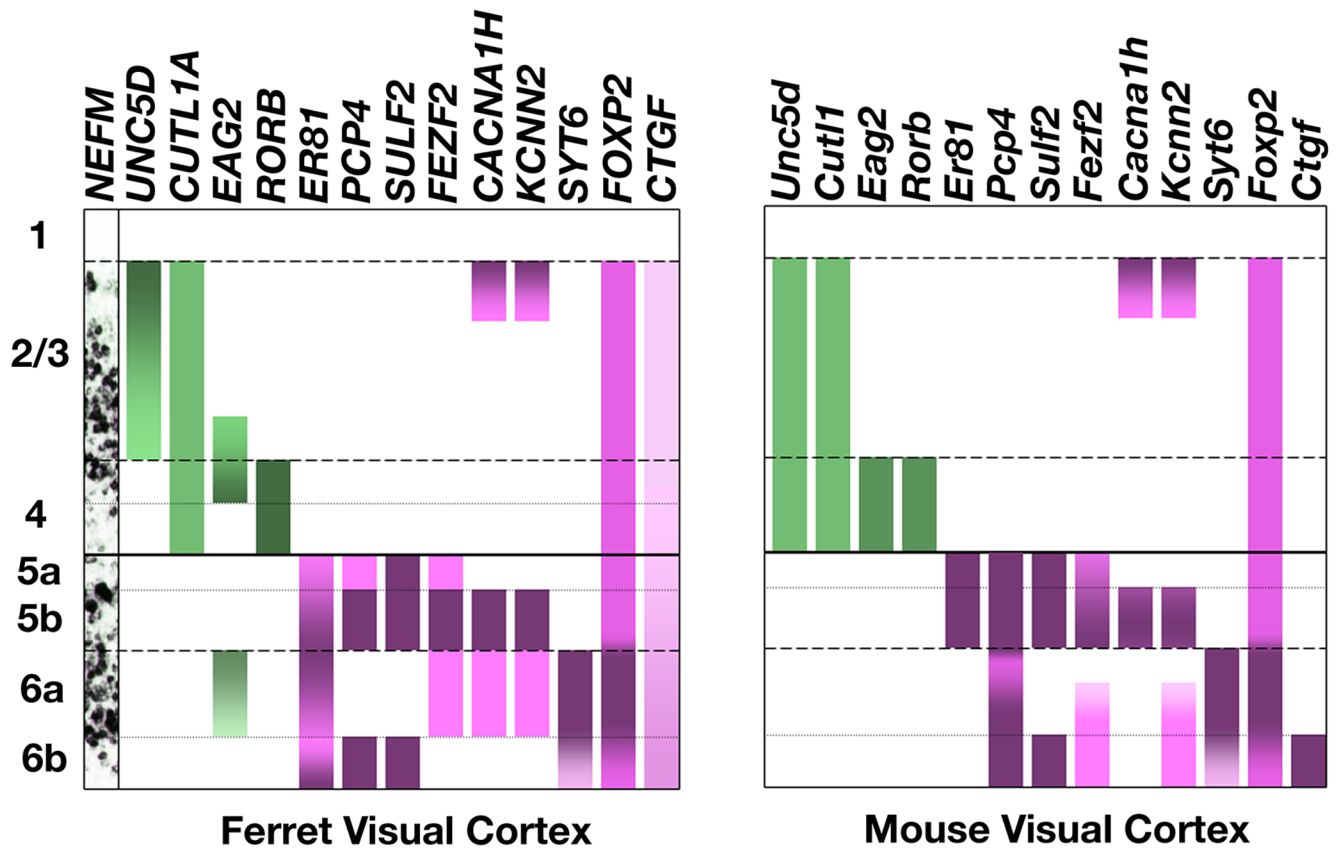


Figure 10. Comparison of ferret and mouse layer marker gene expression profiles for visual cortex

Upper (2 – 4) layer markers are indicated in green, and deep (5,6) layer markers are indicated in magenta. Gene expression patterns in mouse and ferret neocortex are strikingly similar. Note the consistently sharp gene expression boundary between layers 4 and 5 in both species.

Table 1
Molecular markers for ferret neocortical expression analysis

Candidate ferret layer markers were chosen based on gene expression patterns seen in rodent cerebral cortex.

Gene	Encoding Protein Product	Expression in Rodent Cortex	Rodent Cortex References
<i>ELAVL3/HUC</i>	Neuron-specific RNA binding protein	Pan-neuronal	Okano and Darnell, 1997
<i>VGLUT1/SLC17A7</i>	Vesicular glutamate transporter	Excitatory neurons	Fremeau et al., 2001
<i>GAD65/GAD2</i>	GABA synthetic enzyme	Inhibitory neurons	Feldblum et al., 1993
<i>NEFM</i>	Middle weight neurofilament	Pyramidal neurons	Hoffman et al., 1987; Kirkcaldie et al., 2002
<i>UNC5D/SVET1</i>	Netrin receptor	Layers 2 – 4	Tarabykin et al., 2001
<i>CUX1/CUTL1</i>	Homeodomain transcription factor	Layers 2 – 4	Nieto et al., 2004
<i>EAG2/KCNH5</i>	Potassium channel	Layer 4	Ludwig et al., 2000; Saganich et al., 2001
<i>RORB/NR1F2</i>	Nuclear receptor transcription factor	Layer 4	Schaeren-Wiemers et al., 1997
<i>MDGA1</i>	MAM-domain, GPI anchored	Layer 4	Takeuchi et al., 2007
<i>ER81/ETV1</i>	ETS transcription factor	Layer 5	Hevner et al., 2003
<i>PCP4</i>	Small peptide of unknown function	Layer 5	Bulfone et al., 2004
<i>SULF2</i>	Heparan sulfatase	Layer 5	Nagamine et al., 2005
<i>FEZF2/ZNF312</i>	Zinc finger transcription factor	Layer 5	Inoue et al., 2004
<i>KCNN2/SK2/KCa2.2</i>	Potassium channel	Layer 5	Sailer et al., 2002
<i>CACNA1H/Cav3.2</i>	Calcium channel	Layer 5	Talley et al., 1999
<i>SERPINE2</i>	Serpin peptidase inhibitor (nexin)	Layer 5	Reinhard et al., 1994
<i>SYT6</i>	Synaptotagmin 6	Layer 6	Ullrich and Sudhof, 1995
<i>FOXP2</i>	Forkhead transcription factor	Layer 6	Shu et al., 2001
<i>CTGF</i>	Connective tissue growth factor	Layer 6b	Heuer et al., 2003